A&A 421, 1131–1142 (2004)
DOI: 10.1051/0004-6361:20040319

Astronomy & Astrophysics

On the mass transfer in AE Aquarii

N. R. Ikhsanov[1,3,4], V. V. Neustroev[2,5], and N. G. Beskrovnaya[3,4]

[1] Korea Astronomy Observatory, 61-1 Whaam-dong, Yusong-gu, Taejon 305-348, Republic of Korea
[2] Computational Astrophysics Laboratory, National University of Ireland, Galway, Newcastle Rd., Galway, Ireland
[3] Central Astronomical Observatory of the Russian Academy of Sciences, Pulkovo 65/1, 196140 St. Petersburg, Russia
[4] Isaac Newton Institute of Chile, St. Petersburg Branch, Russia
[5] Isaac Newton Institute of Chile, Kazan Branch, Russia

Received 24 February 2004 / Accepted 30 March 2004

Abstract. The observed properties of the close binary AE Aqr indicate that the mass transfer in this system operates via the Roche lobe overflow mechanism, but the material transferred from the normal companion is neither accreted onto the surface of the white dwarf nor stored in a disk around its magnetosphere. As previously shown, such a situation can be realized if the white dwarf operates as a propeller. At the same time, the efficiency of the propeller action by the white dwarf is insufficient to explain the rapid braking of the white dwarf, which implies that the spin-down power is in excess of the bolometric luminosity of the system. To avoid this problem we have simulated the mass-transfer process in AE Aqr assuming that the observed braking of the white dwarf is governed by a pulsar-like spin-down mechanism. We show that the expected Hα Doppler tomogram in this case resembles the tomogram observed from the system. We find that the agreement between the simulated and the observed tomograms is rather good provided the mean value of the mass-transfer rate $\langle \dot{M} \rangle \sim 5 \times 10^{16}$ g s^{-1}. Three spatially separated sources of Hα emission can be distinguished within this approach. The structure of the tomogram depends on the relative contributions of these sources to the Hα emission and is expected to vary from night to night.

Key words. stars: novae, cataclysmic variables – magnetic fields – stars: pulsars: general – stars: white dwarfs – X-rays: binaries – stars: individual: AE Aqr

1. Introduction

AE Aquarii is a peculiar nova-like star at a distance of $\sim$100 $\pm$ 30 pc (Welsh et al. 1995; Friedjung 1997). It is a non-eclipsing close binary system with an orbital period $P_{\rm orb} \approx 9.88$ h and orbital eccentricity $e \approx 0.02$ (Chincarini & Walker 1981). The normal companion (secondary) is a K3–K5 red dwarf on or close to the main sequence (Bruch 1991; Welsh et al. 1995). The primary is a magnetized white dwarf rotating with the period $P_{\rm s} \approx 33$ s (Patterson 1979; Eracleous et al. 1994). The inclination angle of the system and the mass ratio are limited to $50^\circ < i < 70^\circ$, and $0.58 \lesssim (q = M_2/M_1) \lesssim 0.89$, respectively, and the mass of the white dwarf is evaluated as $0.8 \lesssim M_1 \lesssim 1\ M_\odot$ (Reinsch & Beuermann 1994; Welsh et al. 1995).

The system emits detectable radiation in almost all parts of the spectrum. It is a powerful non-thermal flaring radio source (Bastian et al. 1988; Meintjes & Venter 2003, and references therein) and, possibly, the source of very high energy γ-rays (Bowden et al. 1992; Meintjes et al. 1994; see, however, Lang et al. 1998). The optical, UV, and X-ray radiation of the system is predominantly thermal and comes from at least three different sources. The visual light is dominated by the secondary (Bruch 1991; Welsh et al. 1995). The contribution of the primary is observed mainly in the form of 33 s (and 16.5 s) coherent oscillations detectable in the optical, UV, and X-rays (Patterson 1979; Eracleous et al. 1994; Patterson et al. 1980). The remaining light comes from a highly variable extended source, which manifests itself in the blue/UV continuum, the optical/UV broad single-peaked emission lines, and the non-pulsing X-ray component. This source is associated with the mass-transfer process and is suspected of being responsible for the peculiar rapid flaring of the star (for discussion see e.g., Eracleous & Horne 1996).

AE Aqr is currently assigned to the DQ Her subclass of magnetic Cataclysmic Variables (CVs). The members of this subclass are interacting low-mass close binaries, in which the degenerate companions are magnetized white dwarfs rotating with periods $P_{\rm s} \ll P_{\rm orb}$ and accreting material from a Keplerian disk (see e.g., Warner 1995). However, extensive investigations during the last decade have clearly shown that AE Aqr does not fit in this model. Namely, studies of the 33 s pulsations in the optical/UV (Eracleous et al. 1994) and X-rays (Reinsch et al. 1995; Clayton & Osborne 1995; Choi et al. 1999) revealed that the contribution of the white dwarf to the system radiation is significantly smaller than previously assumed within the

Send offprint requests to: N. R. Ikhsanov,
e-mail: ikhsanov@kao.re.kr

accretion-powered white dwarf model. Furthermore, analysis of the Hα Doppler tomogram of AE Aqr has shown no evidence of an accretion disk in the system (Wynn et al. 1997; Welsh et al. 1998). Finally, de Jager et al. (1994) reported a mean spin-down rate of the white dwarf $\dot{P}_0 = 5.64 \times 10^{-14}$ s s^{-1}. The remarkable stability of the observed braking over the span of 14.5 yr suggests that the entire white dwarf is spinning down (for a detailed discussion see Welsh 1999). This allows us to evaluate the spin-down power of the white dwarf as

$$L_{\rm sd} = 6 \times 10^{33}\ I_{50}\ P_{33}^{-3}\ (\dot{P}/\dot{P}_0)\ {\rm erg\ s^{-1}}, \quad (1)$$

where I_{50} and P_{33} are the moment of inertia and the spin period of the white dwarf expressed in units of 10^{50} g cm^2 and 33 s, respectively. $L_{\rm sd}$ exceeds the luminosity of the system observed in the UV and X-rays by a factor of 120–300 and even the bolometric luminosity by a factor of more than 5 (hereafter, the distance to the star is adopted as 100 pc). This indicates that the spin-down power dominates the system energy budget and raises a question about the form in which this energy is released.

Among possible answers to this question the following two are currently under discussion. The first, a so called "magnetic propeller" model, was presented by Wynn et al. (1997), who suggested that the rotation rate of the white dwarf decelerates by means of interaction between its fast rotating magnetosphere and the material inflowing from the secondary. The second, a so called "pulsar-like white dwarf" model, was suggested by Ikhsanov (1998), who indicated that the observed braking of the white dwarf could be explained in terms of the canonical pulsar-like spin-down mechanism (Pacini 1968; Goldreich & Julian 1969), provided its surface magnetic field is 50 MG. In this paper we address the comparative analysis of these models. The basic statements of these approaches are briefly discussed in the following two sections. In Sect. 4 we present the results of our simulation of the Hα Doppler tomogram of AE Aqr. The adopted assumptions are summarized in Sect. 5. The basic conclusions are given in Sect. 6.

2. Propeller action by the white dwarf

The observed properties of the optical/UV emission lines unambiguously indicate that a relatively intensive mass-transfer takes place between the system components of AE Aqr. In particular, the narrow component of the Balmer emission lines is nearly in anti-phase to the absorption lines of the red dwarf (Reinsch & Beuermann 1994), that suggests its origin is near the white dwarf. Furthermore, the evaluated velocity and luminosity of the emission line source are significantly larger than those typically expected in the wind of red dwarfs (see e.g., Eracleous et al. 1994).These properties speak in favor of an association of the emission line source with the material transferred from the normal component through the Roche lobe of the white dwarf.

The rate of mass transfer in AE Aqr is still a subject of discussion. A lower limit to this parameter can be derived assuming that the radiation of emission lines is generated inside the Roche lobe of the white dwarf and is powered by the accretion energy. In this case one finds $\dot{M} > 10^{15} L_{31} R_{10} M_{0.9}^{-1}$ g s^{-1}, where L_{31} is the luminosity of the emission line source (see e.g. Table 3 in Eracleous & Horne 1996), and $M_{0.9}$ is the mass of the white dwarf in units of 0.9 $M_\odot$. R_{10} is the distance of the closest approach of the material responsible for the observed emission lines to the white dwarf expressed in units of 10^{10} cm. This parameter can be limited using the expression $R \lesssim GM_{\rm wd}/V_{\rm em}^2$, where $V_{\rm em}$ is the velocity of the emitting material derived from the observed width of the emission lines.

The above limit to $\dot{M}$ represents the minimum possible value of the mass-transfer rate in AE Aqr and, as will be shown below, is significantly underestimated. Nevertheless, this estimate plays an important role in the identification of the mass-transfer mechanism. Indeed, the derived value exceeds the maximum possible rate of mass capture by the white dwarf from the wind of its companion by more than three orders of magnitude (Ikhsanov 1997). This justifies that the mass-transfer in AE Aqr operates via the Roche lobe overflow mechanism and hence, the secondary overflows its Roche lobe and loses material through the L1 point towards the primary.

However, a relatively low X-ray luminosity of AE Aqr ($L_{\rm x} \sim 10^{31}$ erg s^{-1}, see e.g. Choi et al. 1999) and the structure of the Hα Doppler tomogram derived by Wynn et al. (1997) and Welsh et al. (1998) argue against the possibility that the material transferred from the red dwarf is either accreted onto the surface of the white dwarf or stored in a disk. To solve this paradox the hypothesis has been invoked that the material flowing into the Roche lobe of the white dwarf is ejected from the system without forming a disk.

An effort to reconstruct the mass-transfer picture within this hypothesis was first made by Wynn et al. (1997). They modelled the stream as a set of diamagnetic blobs, which move through the fast rotating magnetosphere of the primary, interacting with the local magnetic field via a surface drag term. In this case, the trajectories of the blobs differ from the ballistic case, and the stream is able to leave the system without forming a disk if the magnetic moment of the primary is $\mu \gtrsim 10^{32}$ G cm^3. In particular, putting $\mu \simeq 10^{32}$ G cm^3 (i.e. within the expected range of the magnetic moments of Intermediate Polars), Wynn et al. (1997) found that blobs reach the escape (maximum) velocity of $V_{\rm esc} \lesssim 1000$ km s^{-1} at the closest approach to the white dwarf, $r_0 \gtrsim 10^{10}$ cm, and leave the system without forming a disk with an average velocity $V_\infty \sim 300$ km s^{-1}. The ejection of material in this scenario occurs due to propeller action by the white dwarf, which is also assumed to be responsible for the observed braking of the primary.

The Hα Doppler tomogram calculated within this model is similar to the tomogram observed in AE Aqr in several important aspects. In particular, neither shows azimuthal symmetry, and the emission is not centered on the white dwarf but is primarily in the lower-left quadrant (V_x, V_y both negative). These similarities indicate that the picture reconstructed by Wynn et al. (1997) is qualitatively correct.

At the same time, some of the quantitative predictions of the "magnetic propeller" model have not been observationally confirmed. As shown by Welsh et al. (1998), the observed tomogram does not contain the high velocity "loop" ($|V| \sim 700$–1000 km s^{-1}) predicted by Wynn et al. (1997, see

Fig. 3), and on the other hand it shows that the contribution of material at low velocities ($|V| \lesssim 100$ km s^{-1}) is significantly larger than expected from the simulated picture. These inconsistencies forced Welsh et al. (1998) to suggest that the heating of the blobs, when they pass the acceleration region at their closest approach to the white dwarf, is negligible, and therefore that their contribution to the Hα emission of the system is small. Following this assumption they have placed the region of energy release outside the Roche lobe of the primary where the trajectories of blobs of different masses cross each other and collisions of the ejected blobs can be expected. However, as mentioned by Welsh (1999), some of the properties of AE Aqr (such as the large velocities in the emission lines during flares and the existence of high-excitation emission lines) remain puzzling even in this so called "colliding blobs" scenario.

Another difficulty with the "magnetic propeller" model has been mentioned by Ikhsanov (1998), Meintjes & de Jager (2000), and Choi & Yi (2000). As they have shown, the efficiency of the propeller action by the white dwarf under the conditions of interest is not sufficient to explain the observed rapid braking of the primary. Indeed, following Wynn et al. (1997) one could assume that almost all spin-down power of the white dwarf is transferred into the kinetic energy of the ejected material. However, the kinetic luminosity of the ejected blobs is obviously limited to

$$L_{\rm kin} \lesssim (1/2)\dot{M}V_{\rm esc}^2 \simeq 5\times10^{32}\dot{M}_{17}\,V_8^2 \ {\rm erg\,s^{-1}}, \qquad (2)$$

where $V_8 = V_{\rm esc}/10^8$ cm s^{-1} and $\dot{M}_{17}$ is the mass transfer rate expressed in units of 10^{17} g s^{-1}. Hence, for this assumption to be satisfied, the mass transfer rate in the system should be in excess of 10^{18} g s^{-1}, which is inconsistent with the value of $\dot{M}$ derived from observations (see e.g., Eracleous & Horne 1996). On the other hand, the assumption that a significant part of the spin-down power is transferred into the thermal energy of the ejected gas contradicts the derived value of the ratios $L_{\rm UV}/L_{\rm sd} \sim L_{\rm x}/L_{\rm sd} \ll 1$. Therefore, the question about the nature of the observed braking of the white dwarf within the "magnetic propeller" model remains open.

The problems mentioned above indicate that the "magnetic propeller" model cannot provide us with a complete picture of AE Aqr, and an improvement of this model is required. They also show that the problem that should be addressed first in any further improvements is the spin-down mechanism of the white dwarf. As long as this problem remains unsolved, the form in which the spin-down power is released turns out to be unclear, and therefore, the major part of the energy released in the system is not taken into account.

At the same time, for a solution of the spin-down problem to be reliable it should also meet the diskless mass-transfer criteria. In this light, the improvement suggested by Meintjes & de Jager (2000) cannot be applied to the interpretation of AE Aqr, since their approach requires the existence of a clumpy disk around the white dwarf. On the other hand, the model of Choi & Yi (2000), in which the spin-down power is assumed to be spent in the emission of gravitational waves, cannot be accepted either. Although the mass-transfer picture within this model is similar to that reconstructed by Wynn et al. (1997), the adopted mass distribution over the primary surface is unreliable (for a detailed discussion see Ikhsanov & Beskrovnaya 2002). Among the improvements of the "magnetic propeller" model so far discussed in the literature, only the pulsar-like spin-down model meets the criteria. The reliability of this improvement is discussed in the following section.

3. Pulsar-like spin-down

The hypothesis of pulsar-like spin-down of the white dwarf in AE Aqr has a certain observational basis. A situation in which the spin-down power of a star exceeds its bolometric luminosity significantly is unique for CVs as well as for all presently known accretion-powered sources. At the same time, this situation is typical for the spin-powered pulsars, whose luminosity constitutes only a small fraction ($\sim10^{-3}$–10^{-1}) of their spin-down power (for a review see Manchester & Taylor 1977; Hartmann 1995). Furthermore, while the appearance of AE Aqr in X-rays is very atypical for the accretion-powered white dwarfs (Clayton & Osborne 1995), it resembles the appearance of spin-powered pulsars observed in the ROSAT energy range (see e.g., Becker & Trümper 1997). For instance, the X-ray spectrum is significantly softer than those typically observed from accretion-powered compact stars, and the ratio of the luminosity of the pulsing component to the spin-down power is close to 10^{-3}. Finally, as reported by Meintjes et al. (1994), the intensity of the very high energy γ-ray emission detected from AE Aqr significantly exceeds the intensity of radiation emitted in other parts of the spectrum. Such behavior is also typical for spin-powered pulsars (see e.g., Tompson 1996) and is consistent with modern views on the processes of energy release in these sources (for a review see Michel 1991). Thus, the investigation of the hypothesis that the braking of both the white dwarf in AE Aqr and the spin-powered pulsars is governed by the same mechanism appears to be quite reasonable.

As shown by Ikhsanov (1998), for this hypothesis to be effective the dipole magnetic moment of the white dwarf should be as large as

$$\mu \simeq 1.4\times10^{34}\,P_{33}^2\left(\frac{L_{\rm sd}}{6\times10^{33}\ {\rm erg\,s^{-1}}}\right)^{1/2} {\rm G\,cm^3}. \qquad (3)$$

This implies that the mean strength of the magnetic field at the surface of the white dwarf is $B(R_{\rm wd}) \approx 50$ MG. Under these conditions the spin-down power is spent in the generation of magneto-dipole waves and particle acceleration and hence is released mainly in undetectable parts of the spectrum. Therefore, the observed inequality $L_{\rm bol} < L_{\rm sd}$ turns out to be naturally explained within this approach.

The limitation of the magnetic field to 50 MG is consistent with present views on possible values of the surface field strength of white dwarfs (see e.g., Jordan 2001). In particular, the magnetic field of white dwarfs in Polars is of the same order of magnitude (Cropper 1990; Chanmugam 1992). However, it is significantly above the previous limit to the strength of the magnetic field of the white dwarf in AE Aqr derived by Bastian et al. (1988) and Stockman et al. (1992) from the analysis of the circularly polarized optical emission.

The reason for this inconsistency has recently been investigated by Ikhsanov et al. (2002). As they have shown, the

limitation presented by Bastian et al. (1988) and Stockman et al. (1992) is model-dependent and is based on the assumption that the radiation of the white dwarf is powered mainly by the accretion of material onto its surface. However, the investigations of AE Aqr in the UV (Eracleous et al. 1994) and X-rays (Clayton & Osborne 1995; Choi et al. 1999) have clearly shown that this assumption is not valid. As presently recognized, the contribution of the hot polar caps to the visual radiation of AE Aqr does not exceed 0.1%–0.2%. In this situation the hot polar caps cannot be the source responsible for the circularly polarized radiation observed from the system. Otherwise, the intrinsic polarization of the source proves to be in excess of 100%, that is obviously impossible (see Ikhsanov et al. 2002). Therefore, the above mentioned inconsistency cannot be used as an argument to reject the possibility of the white dwarf in AE Aqr having a magnetic field as strong as 50 MG.

A possible history of AE Aqr within the pulsar-like model is more complicated than that usually modelled within the "magnetic propeller" approach (Meintjes 2002; Schenker et al. 2002). Indeed, a white dwarf with mass 0.9 $M_\odot$ and surface magnetic field 50 MG can only be spun up to the period of 33 s if the mass transfer rate during a previous epoch was in excess of the Eddington limit ($\sim 3 \times 10^{21}$ g s^{-1}) by a factor of 3. Accretion with these characteristics resembles the process of the merging of a white dwarf with another star rather than the mass exchange between a main sequence red dwarf and a white dwarf in a close binary. The formation of a fast rotating, strongly magnetized white dwarf due to its merging with a companion has been already discussed by Paczyński (1990). Following this scenario, one should assume that the white dwarf in AE Aqr is a product of the merging of a magnetized white dwarf and, possibly, a brown dwarf of mass $\sim 0.03\ M_\odot$.

However, as pointed out by Ikhsanov (1999), the process of merging is not the only possible solution. An alternative explanation is based on the scenario of magnetic field amplification in very fast rotating compact stars (Kluźniak & Ruderman 1998; Spruit 1999). According to Chanmugam et al. (1987), the rotation of a white dwarf with mass $M_{\rm wd} = 0.9\ M_\odot$ becomes significantly non-uniform as its period decreases below $P_{\rm cr} \simeq 20$ s. The magnetic field inside the star in this state is winding up to $\sim 10^9$ G on a time scale of a month, and manifests itself at the surface due to the buoyant instability producing a surface field of $\sim 10^8$ G. This allows us to envisage a situation in which the magnetic field of the white dwarf in AE Aqr was amplified to its present value during the last stage of a previous accretion-driven spin-up epoch. As shown by Ikhsanov (1999), for this scenario to be effective one has to assume that the initial magnetic moment of the white dwarf was

$$\mu_0 \lesssim 2 \times 10^{31}\ \dot{M}_{17}^{1/2}\ P_{20}^{7/6}\ M_{0.9}^{5/6}\ {\rm g\,s^{-1}},$$

which implies that in a previous epoch AE Aqr was an ordinary member of the DQ Her subclass of CVs.

Although both of the above mentioned scenarios lead to a rather complicated history of AE Aqr, it is clear that a solution of this problem within the pulsar-like spin-down model is not impossible. A more precise investigation, however, is not effective as long as the presently observed stage of the system is not well identified. Therefore, in this paper we will focus mainly on the analysis of currently observed properties of AE Aqr.

The natural solution of the spin-down problem is not the only advantage of the pulsar-like model. It also gives a reasonable explanation of some properties of AE Aqr observed in the high-energy parts of the spectrum. In particular, it predicts the maximum energy of particles accelerated by the white dwarf $E_{\rm p}^{\rm max} \sim 2 \times 10^{12}$ eV (see Eq. (10) in Ikhsanov 1998). This prediction is consistent with the characteristics of the TeV γ-ray events observed from the system (Meintjes et al. 1994). Furthermore, it also allows us to associate the origin of the pulsing UV and X-ray emission with the processes of non-thermal energy release in the magnetosphere of the white dwarf, i.e. particle acceleration in the inner (and, possibly, outer) gap and, correspondingly, the impact of particles responsible for the back-flowing current onto the surface of the white dwarf at the magnetic pole regions (for a discussion see Ikhsanov 1998, and references therein). The latter process should lead to the heating of the surface of the white dwarf, while the radiative losses of relativistic electrons are expected to be observed in the X-ray part of the spectrum. Under these conditions, the luminosity of pulsing emission in the UV would be comparable with that of the pulsing X-ray component, and the area of the hot polar caps can be limited to (see Eq. (11) in Ikhsanov 1998)

$$A_{\rm pc} \lesssim 3 \times 10^{16}\ \eta_{0.37}^{-1}\ \dot{M}_{16.5}^{2/7}\ \mu_{34.2}^{-4/7}\ R_{8.8}^{3}\ M_{0.9}\ {\rm cm^2}, \qquad (4)$$

where $\mu_{34.2}$ and $R_{8.8}$ are the magnetic moment and the radius of the white dwarf expressed in units of $10^{34.2}$ G cm^3 and $10^{8.8}$ cm, respectively. $\eta_{0.37} = \eta/0.37$ is the parameter accounting for the geometry of the accretion flow, which in the case of a stream is normalized following Hameury et al. (1986).

Both of these predictions are in good agreement with corresponding properties of AE Aqr (see e.g., Eracleous et al. 1994; Choi et al. 1999), and they allow us to avoid a very controversial assumption about the accretion nature of the pulsing UV and X-ray radiation of AE Aqr (for a discussion see Choi et al. 1999; Ikhsanov 2001).

Finally, the pulsar-like model naturally leads to a conclusion about the diskless mass transfer in the system. Indeed, within this approach the Alfvén radius of the white dwarf,

$$R_{\rm A} \simeq 3 \times 10^{10}\ \eta_{0.37}\ \mu_{34.2}^{4/7}\ \dot{M}_{17}^{-2/7}\ M_{0.9}^{-1/7}\ {\rm cm}, \qquad (5)$$

is larger than the circularization radius for all reasonable values of $\dot{M}$. This means that diskless mass transfer in the system is realized, and moreover, this is expected independently of whether the stream transferred through the L1 point is initially homogeneous or inhomogeneous. In this case the assumption that the stream disintegrates into blobs before the point of its closest approach to the white dwarf (as adopted by Wynn et al. 1997) turns out to be unnecessary. Instead, one can envisage a scenario in which the stream disintegration occurs in the vicinity of the Alfvén surface of the white dwarf, where such a disintegration, according to Arons & Lea (1980), is expected. However, is the Hα Doppler tomogram expected within this scenario consistent with the tomogram observed from the system? The analysis of this question is addressed in the next section.

4. Simulation of Hα Doppler tomogram

We consider a situation in which the secondary star overflows its Roche lobe and loses material in the form of a stream through the L1 point. The stream flows into the Roche lobe of the white dwarf at the speed of sound and initially follows a ballistic trajectory. Following Wynn et al. (1997), we assume that at a certain point (its location depends on the scenario considered) the stream disintegrates into a set of large diamagnetic blobs. The blobs interact with the magnetospheric field of the white dwarf via the drag term. Due to this interaction their trajectories are modified by the magnetic acceleration

$$g_{\rm mag} = -k[V - V_{\rm f}]_{\perp}, \tag{6}$$

where $k \sim B^2/c_{\rm A}\rho_{\rm b}l_{\rm b}$ is the drag coefficient, V and $V_{\rm f}$ are the blob and field velocities, and the suffix $\perp$ denotes the velocity component perpendicular to the field lines. $c_{\rm A}$ is the Alfvén speed in the interblob plasma, which under the conditions of interest can be approximated by the speed of light. $\rho_{\rm b}$ and $l_{\rm b}$ are the density and radius of the blobs.

As shown by Wynn & King (1995), the drag coefficient can be expressed in the form $k \sim k_0(r/r_0)^{-n}$, where k_0, n, and r_0 are constants. Setting $\rho_{\rm b}(r_0) = 10^{-11}\rho_{-11}$ g cm^{-3} and $l_{\rm b}(r_0) = 10^9 l_9$ cm we evaluate the parameter k_0 as (for discussion see Wynn et al. 1997)

$$k_0 \simeq 3.3\times10^{-9}\, B^2(r_0)\,\rho_{-11}^{-1}\, l_9^{-1}\ {\rm s}^{-1}. \tag{7}$$

Simulating the trajectory of the material within the Roche lobe of the white dwarf we have assumed that the drag interaction between the stream and the magnetic field of the primary before the point of the stream disintegration is small and therefore, the stream before this point follows a ballistic trajectory. This assumption is reasonable if the point of the stream disintegration is located at a distance $r \gtrsim R_{\rm circ}$, where $R_{\rm circ}$ is the circularization radius, which is about 2.5×10^{10} cm for the parameters of AE Aqr (see Eq. (4.17) in Frank et al. 1985). Starting with the point at which the stream disintegrates into blobs the drag term becomes important and therefore, the trajectories of the blobs deviate significantly from the ballistic ones. Following this method, we have performed several runs of calculations placing the point of disintegration at the L1 point, at the point of the closest approach of the stream to the white dwarf, r_0, and at a few intermediate points located within the interval [L1, r_0]. This scheme of calculations has been applied to both the "magnetic propeller" and the "pulsar-like white dwarf" approaches. The results of our simulations are presented in the following two subsections.

4.1. The magnetic propeller approach

To test the consistency of the results of our calculations with those previously derived by other authors we have simulated the trajectories of blobs using the parameters of AE Aqr adopted by Wynn et al. (1997) as follows. System parameters: mass ratio $q = 0.64$, orbital period $P_{\rm orb} = 9.9$ h, and inclination angle $i = 55°$, and parameters of the white dwarf: mass $M_1 = 0.9\ M_\odot$, dipole magnetic moment $\mu = 10^{32}$ G cm^3, and spin period $P_{\rm s} = 33$ s. The stream of material transferred from the secondary has been modelled as a set of diamagnetic blobs. The distance to the point of the stream disintegration has been assumed to satisfy the condition $r_{\rm dis} \gg R_{\rm circ}$. The radius and the density of blobs at their closest approach to the white dwarf have been taken as $l_{\rm b} = 10^9\, l_9$ cm and $\rho_{\rm b} = 10^{-11}\,\rho_{-11}$ g cm^{-3}, respectively. The value of the parameter n has been chosen to be $n = 2$. Finally, the parameter r_0 has been limited to $r_0 \gtrsim R_{\rm min}$, where

$$R_{\rm min} \simeq 10^{10}\left(\frac{q}{0.64}\right)^{-0.464}\left(\frac{a}{1.8\times10^{11}\ {\rm cm}}\right)\ {\rm cm} \tag{8}$$

is the distance of the closest approach of a homogeneous stream to the white dwarf (see Eq. (2.14) of Warner 1995).

The trajectories of the blobs and the expected Hα Doppler tomogram simulated under these conditions are shown in Fig. 1. The best fit to the observed tomogram is found for $k_0 \simeq (0.8\text{–}1.3)\times10^{-5}$ s^{-1}. Lines 1–4 represent the trajectories of blobs of different mass with the mass of the blobs decreasing from line 1 to line 4. The more massive the blob the smaller the distance to which it approaches the white dwarf. The trajectories of blobs of different masses intersect beyond the Roche lobe of the white dwarf and, therefore, collisions of the ejected blobs in this region can be expected. The location of the collision zone is shown in panels a and b of Fig. 1 as a hatched region. This region represents the expected structure of the Hα Doppler tomogram within the "colliding blobs" model. The structure of the tomogram derived within the approach of Wynn et al. (1997), i.e. under the assumption that the Hα emission comes mainly from blobs moving through the Roche lobe of the white dwarf, is shown in panel c.

As is easy to see, the derived tomograms are almost identical to those presented by Wynn et al. (1997, see Fig. 3 of their paper) and Welsh et al. (1998, see Fig. 14 of their paper). This proves that our code is working properly and can be used for further analysis.

4.2. The pulsar-like white dwarf approach

The simulation of the stream trajectory within the "pulsar-like" model differs from that in the frame of the "magnetic propeller" model in several important aspects. First, the dipole magnetic moment of the white dwarf within the "pulsar-like" model is assumed to be $\mu \simeq 1.4\times10^{34}$ G cm^3, i.e. a factor of 100 larger than that adopted within the "magnetic propeller" model.

Second, the value of the parameter r_0 is limited to

$$r_0 \gtrsim R_{\rm A} \simeq 3\times10^{10}\,\eta_{0.37}\,\mu_{34.2}^{4/7}\,\dot{M}_{17}^{-2/7}\,M_{0.9}^{-1/7}\ {\rm cm}. \tag{9}$$

This limitation reflects the fact that the magnetic field pressure at the Alfvén radius is strong enough to prevent the stream from approaching the white dwarf closer than $R_{\rm A}$. Within the "magnetic propeller" model $R_{\rm A} < R_{\rm min}$, and hence the pressure by the dipole field of the primary in the radial direction (within the frame centered at the white dwarf) can be neglected. But in the case of the "pulsar-like" model the Alfvén radius of the white dwarf is larger than $R_{\rm min}$. This means that the radial velocity of the inflowing material at $R_{\rm A}$ rapidly drops to zero with corresponding heating and possibly disintegration of the initial

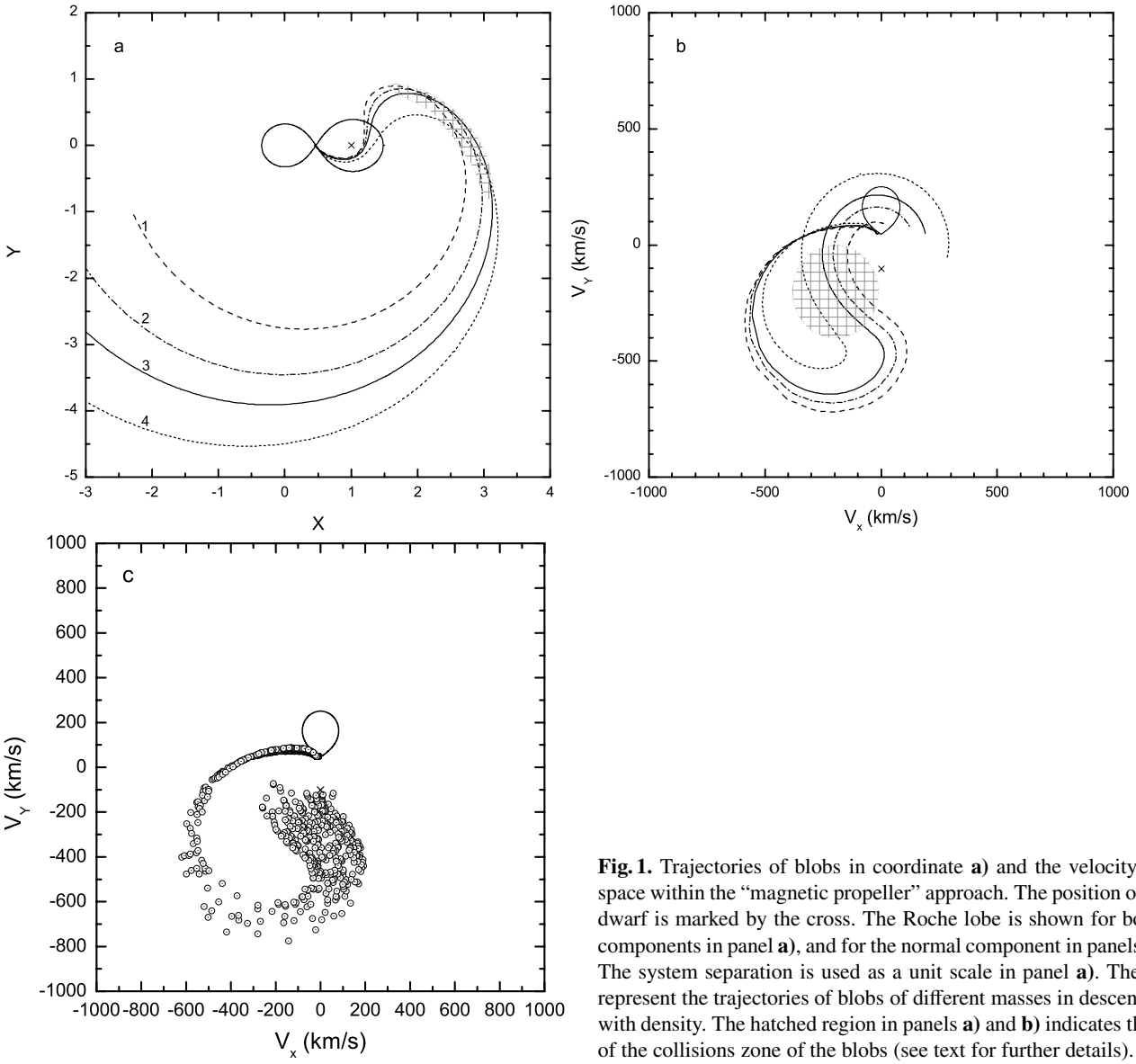

Fig. 1. Trajectories of blobs in coordinate **a)** and the velocity **b)** and **c)** space within the "magnetic propeller" approach. The position of the white dwarf is marked by the cross. The Roche lobe is shown for both system components in panel **a)**, and for the normal component in panels **b)** and **c)**. The system separation is used as a unit scale in panel **a)**. The lines 1–4 represent the trajectories of blobs of different masses in descending order with density. The hatched region in panels **a)** and **b)** indicates the location of the collisions zone of the blobs (see text for further details).

stream. The further trajectory of the material depends on the efficiency of the drag interaction between the blobs and the magnetospheric field of the primary. If this interaction is effective enough for the blobs to be accelerated to the escape velocity in the azimuthal direction, they will leave the system. Otherwise, the material will follow an almost circular orbit around the magnetosphere of the white dwarf.

Finally, the assumption about the stream disintegration at the L1 point within the "pulsar-like" model is not necessary. The point at which the stream disintegrates into diamagnetic blobs in this case can be located anywhere between the L1 point and the Alfvén surface of the primary. As mentioned above, in both cases (homogeneous and inhomogeneous stream) diskless mass transfer is expected within this model. Therefore, parallel to the traditionally considered case of an inhomogeneous stream at the L1 point we also simulated the mass transfer assuming that the point of disintegration of the initially homogeneous stream is located at the Alfvén surface of the primary.

Evaluating the structure of the Hα Doppler tomogram, one should also take into account that a third source of Hα emission (in addition to the stream passing through the magnetosphere of the white dwarf and the region of blob collision) can be expected within the pulsar-like model of AE Aqr. This source is associated with the region where the magneto-dipole waves emitted by the white dwarf are absorbed by the background material surrounding the system. According to Rees & Gunn (1974), the distance to this region, $R_{\rm abs}$, can be found by equating the pressure of the magneto-dipole radiation, $p_{\rm md} = L_{\rm sd}/4\pi cR^2$, with the thermal pressure of the surrounding material, $p_{\rm pl} = (1/2)\rho_\infty V_{\rm s}^2$. The interaction between the waves and the gas leads to the formation of a shock in which the energy of waves is converted into the thermal energy of plasma, radiation, and accelerated particles.

To estimate $R_{\rm abs}$ in AE Aqr, we have taken into account that the circumbinary medium of this system is contributed to mainly by the material ejected due to the propeller action of the white dwarf. As shown by Wynn et al. (1997), this

material flows out within the orbital plane of the system following a spiral. *The position angle of the spiral, however, changes with the orbital motion of the system*. Therefore, the distribution of the material surrounding the system has an azimuthal symmetry. Simulation of the stream-like ejection in the rotating system has shown that a circumbinary disk-like envelope with inner radius $R_{\rm cbe} \gtrsim 5 \times 10^{11}$ cm forms around the system. The mean velocity of the ejected material at this distance is $V_{\rm b}(R_{\rm cbe}) \sim 100$ km s^{-1}, and therefore the derived scale is comparable to $P_{\rm orb} V_{\rm b}(R_{\rm cbe})$.

The thickness of the envelope is determined by the thermal expansion of blobs, and its mean value can be normalized as $Z_0(R_{\rm cbe}) = 10^{10}\, Z_{10}$ cm. This allows us to limit the mean density of the envelope material to

$$\rho_{\rm st} \lesssim 10^{-14}\, l_9^3\, Z_{10}^{-3} \left(\frac{\rho_{\rm b}(r_0)}{10^{-11}\,{\rm g cm^{-3}}}\right) {\rm g\ cm^{-3}}. \quad (10)$$

Under these conditions the distance at which the magneto-dipole waves are absorbed by the material of the envelope can be evaluated as

$$R_{\rm abs} \gtrsim 2 \times 10^{12} \rho_{-14}^{-1/2} V_6^{-1} \left(\frac{L_{\rm sd}}{6 \times 10^{33}\ {\rm erg\ s^{-1}}}\right)^{1/2} {\rm cm}. \quad (11)$$

At this distance the circumbinary envelope occupies about 0.5% of the area of a sphere, and the velocity of the material lies within the interval ~50−150 km s^{-1}. This indicates that the envelope will contribute to the Doppler tomogram of the system at low velocities with intensity $\lesssim 5 \times 10^{-3} L_{\rm sd}$.

The results of the simulation of the stream trajectories within the pulsar-like model of AE Aqr are shown in Figs. 2 and 3. These figures differ in the basic assumption about the location of the region of the stream disintegration to the diamagnetic blobs. Namely, in the first run of the calculations (Fig. 2) this region has been placed at the L1 point, and in the second run we have assumed that the stream disintegration occurs at the Alfvén surface of the primary (Fig. 3). The values of the system parameters (except for μ and r_0) in all calculations were chosen to be the same as those adopted by Wynn et al. (1997).

In both runs the calculations were made for three different values of the mass transfer rate: $\dot{M} = 10^{16}$ g s^{-1} (panel a), $\dot{M} = 5 \times 10^{16}$ g s^{-1} (panel b), and $\dot{M} = 10^{17}$ g s^{-1} (panel c). The value of the parameter η was chosen as 0.5. Panel (d) shows the mean picture of the mass transfer on the time scale of the orbital period of AE Aqr. This picture is derived by taking a superposition of states (a), (b), and (c) with equal weights. The expected mean structure of the Hα Doppler tomogram derived in the first and the second runs are presented at the bottom of Figs. 2 and 3, respectively.

One finds the best agreement between the simulated and the observed tomogram for $\langle \dot{M} \rangle = 5 \times 10^{16}$ g s^{-1}, and for $k_0 = 4.8 \times 10^{-7}$ s^{-1} (assuming the stream to be disintegrated at L1) and $k_0 = 7.4 \times 10^{-7}$ s^{-1} (assuming the stream to be disintegrated at $R_{\rm A}$). Here $\langle \dot{M} \rangle$ denotes the average mass-transfer rate on the time scale of the orbital period. Under these conditions the average value of the Alfvén radius of the white dwarf is $\bar{R}_{\rm A} \simeq 4.9 \times 10^{10}$ cm. This allows us to evaluate the average bolometric luminosity of the stream passing through the magnetosphere as $\bar{L}_{\rm st} \sim (\langle \dot{M} \rangle) G M_{\rm wd} / \bar{R}_{\rm A} \simeq 10^{32}$ erg s^{-1}. This value slightly exceeds the luminosity of the low-velocity source situated beyond the light cylinder of the white dwarf and is close to the average luminosity of the extended component of radiation in AE Aqr evaluated by van Paradijs et al. (1989), and Eracleous & Horne (1996) from the optical and UV observations. The main features of the derived tomograms are discussed in the following section.

4.3. Comparative analysis of the derived tomograms

The tomograms calculated within the "pulsar-like" and the "magnetic propeller" models have a number of similarities. In particular, neither shows azimuthal symmetry, and the emission is not centered on the white dwarf but is primarily in the lower-left quadrant (V_x, V_y both negative). Because of these properties all of the simulated tomograms resemble the Doppler tomogram observed from AE Aqr.

There are, however, several important differences. First, the upper limit to the velocity of the stream at the closest approach to the white dwarf within the pulsar-like model is smaller by a factor of 2 than that within the "magnetic propeller" approach. This means that the emission associated with the stream passing through the magnetosphere within the pulsar-like model is produced at velocities <500 km s^{-1}. Since the blobs have different masses, dispersion of their velocities occurs. Furthermore, the velocity of blobs at their closest approach to the primary depends on the mass-transfer rate. Superposition of these effects leads to a situation in which the contribution of the stream at r_0 appears in the mean Doppler tomogram in the form of a spread loop, which is centered at (-250 km s^{-1}; -350 km s^{-1}) and has the size of $|\Delta V_x| \sim 600$ km s^{-1} and $|\Delta V_y| \sim 400$ km s^{-1}.

The emission at these velocities is present in the observed Hα Doppler tomogram of AE Aqr. This indicates that blobs passing through the magnetosphere within the pulsar-like approach are expected to be hot, and their contribution to the Hα emission of the system is significant for all reliable values of $\dot{M}$. Therefore, the problem of the "missing radiation" from the loop associated with the blob trajectories (mentioned by Welsh et al. 1998) does not occur, as one assumes the surface magnetic field of the white dwarf to be of the order of 50 MG.

The second feature of the tomogram simulated within the pulsar-like approach is the significant contribution of the material situated beyond the light cylinder of the white dwarf. The radiation of this source is emitted at velocities ~ 50−150 km s^{-1} and is powered by the energy of the magneto-dipole waves. The luminosity of this source is almost independent of the variations of the mass transfer rate and is comparable with the luminosity of the stream passing through the magnetosphere at $\dot{M} \sim 5 \times 10^{16}$ g s^{-1}. The contribution of this low-velocity source to the Hα system radiation is seen in the center of the Doppler tomogram as a spread spot of radius ~ 150 km s^{-1}.

An additional, intermediate-velocity source of Hα emission is located at a distance of about 1–3 times the binary separation. This source is associated with the region of possible blob collisions. Our simulations indicate that in both models collision of blobs can occur and that the relative velocity of the colliding blobs is of the order of $V_{\rm b-b} \sim 100$ km s^{-1}.

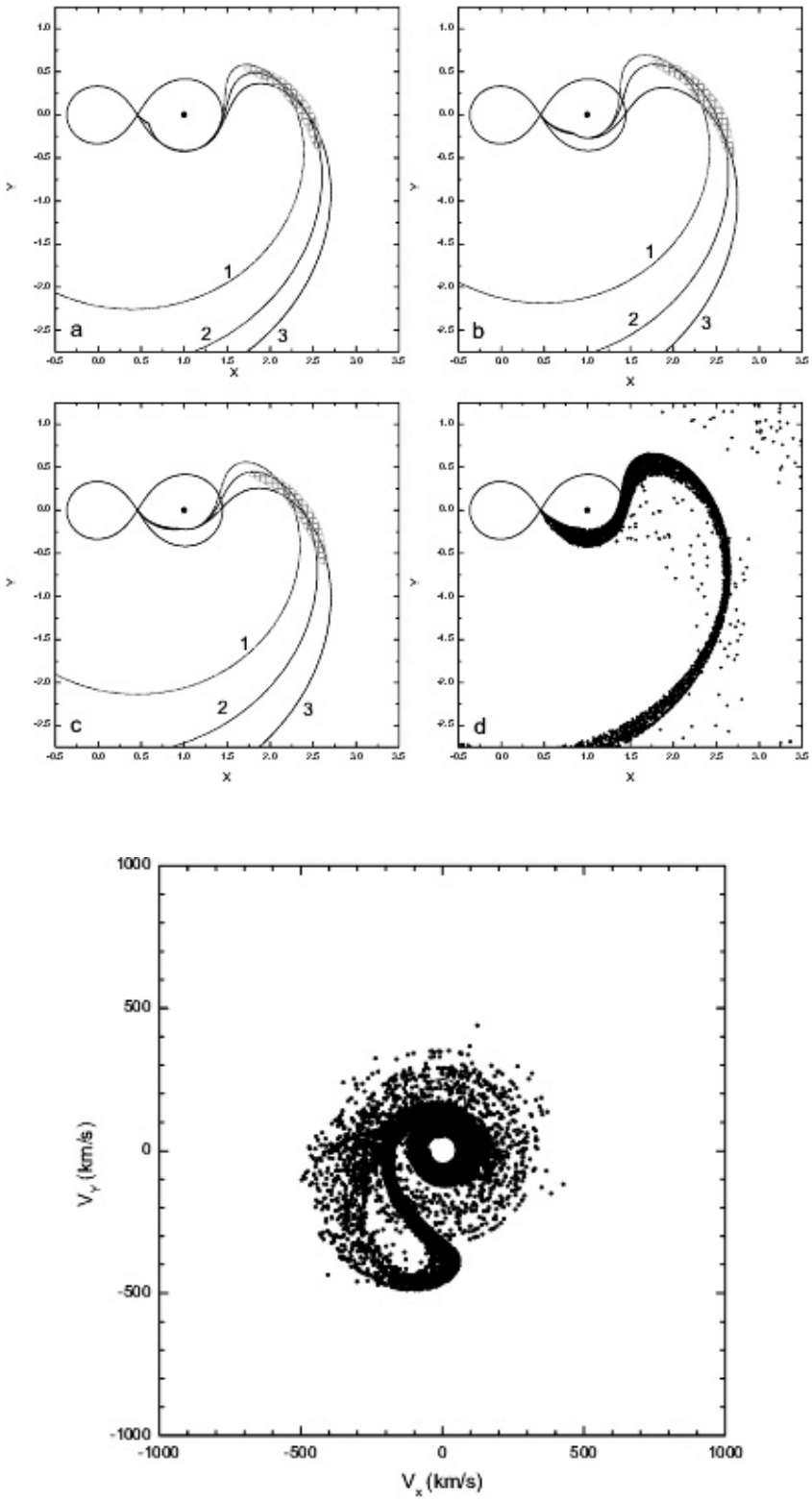

Fig. 2. Trajectories of blobs in the coordinate (*upper panels* **a)–d)**) and the velocity (*bottom panel*) space within the pulsar-like model of AE Aqr. The position of the white dwarf is marked with a black dot. Panels **a)**, **b)**, and **c)** were calculated for mass transfer rates of 10^{16} g s^{-1}, 5×10^{16} g s^{-1}, and 10^{17} g s^{-1}, respectively. The lines in these panels show the trajectories of blobs of different masses. Panel **d)** is the superposition of panels **a)**, **b)**, and **c)** taken with similar weights. The bottom panel represents the expected structure of the Hα Doppler tomogram of the system within this approach. The calculations were made on the assumption that the stream is disintegrated into the blobs at the L1 point. For a detailed description see text.

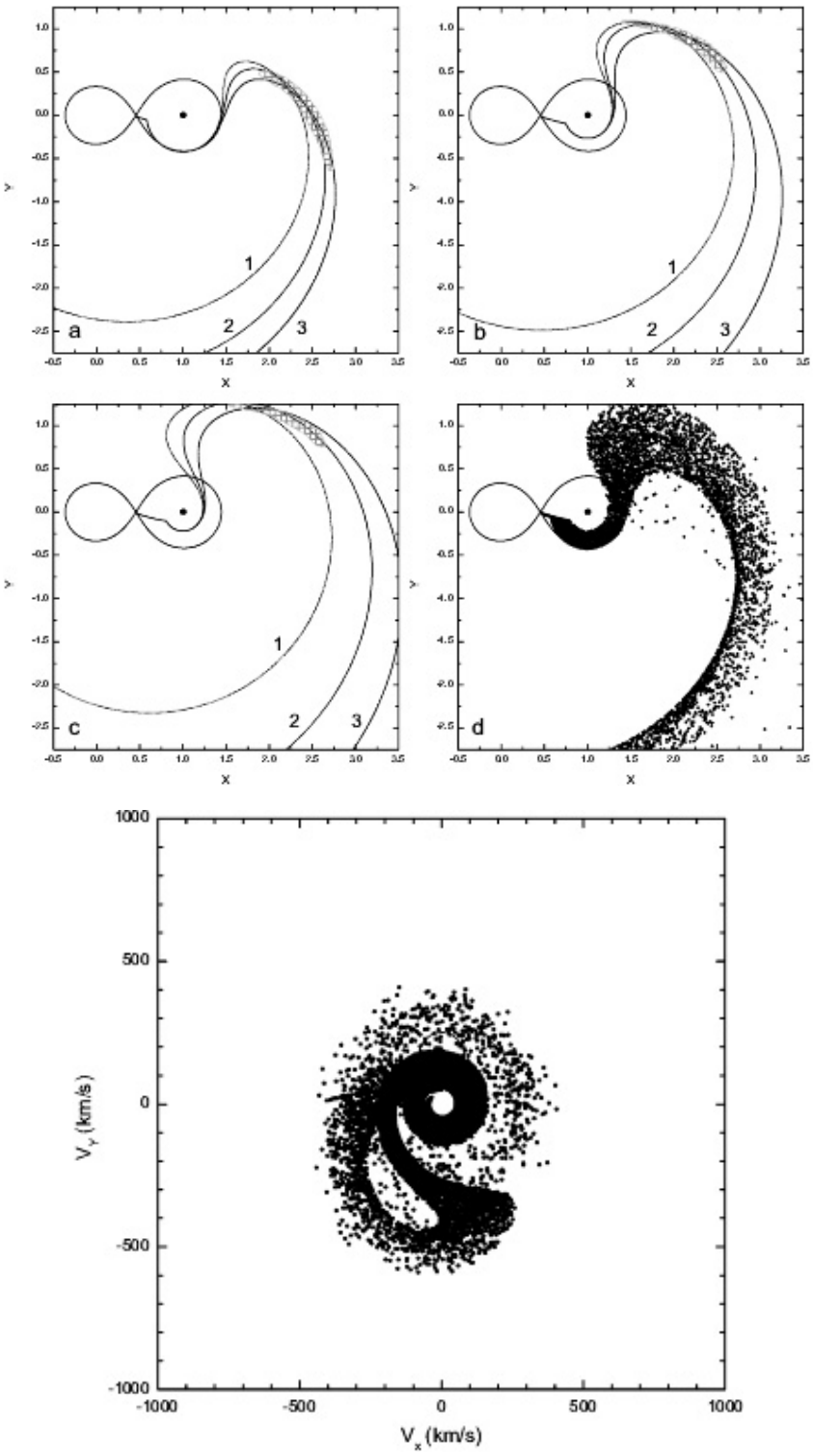

Fig. 3. The same as Fig. 2, except for the assumption that the point of the stream disintegration is located at the Alfvén surface of the white dwarf.

Assuming that all blobs are involved in the collision process, one can limit the rate of energy release in this region to $L_{\rm b-b} \lesssim 5 \times 10^{30} \dot{M}_{17} (V_{\rm b-b}/100\ {\rm km\,s^{-1}})^2\ {\rm erg\,s^{-1}}$. This indicates that the contribution of this source within the pulsar-like model can be significant at relatively high mass-transfer rates but can hardly be recognized when the mass transfer rate drops below $10^{17}\ {\rm g\,s^{-1}}$.

Finally, our simulations have shown that the structure of the tomogram within the pulsar-like model is sensitive to variations in the average mass-transfer rate in the system. As $\langle \dot{M} \rangle$ decreases, the Alfvén radius of the white dwarf becomes larger. In this case the material moving through the magnetosphere turns out to be ejected at smaller velocities, and its contribution to the Hα emission of the system decreases. Therefore, the

tomogram, under these conditions, is dominated by the low velocity component. If, however, $\langle \dot{M} \rangle$ is large during the period of observations, the tomogram is dominated by the "high-velocity spot", which in this case appears in the lower-left quadrant at velocities 350−500 km s^{-1}. Hence, the observed night-to-night variations of the tomogram (see Fig. 10 of Welsh et al. 1998) can be interpreted within the pulsar-like model in terms of the variations of the mass-transfer rate in the system. The range of these variations implies changes in the efficiency of the propeller action by the white dwarf within the interval $\bar{L}_{\rm st}/L_{\rm sd} \sim 0.01$−$0.4$, and therefore, its contribution to the observed braking of the white dwarf remains small.

5. Discussion

It is widely believed that the "magnetic propeller" is the only approach which provides a plausible interpretation of the Hα Doppler tomogram observed in AE Aqr. Following this notion, almost all manifestations of the system during the past 5 years have been discussed solely around the hypothesis that the spin-down of the white dwarf is governed by the propeller spin-down mechanism.

However, as shown in this paper, the Hα Doppler tomogram expected within the pulsar-like approach also resembles the observed tomogram. Furthermore, the agreement between the expected and the observed tomograms within this approach turns out to be even better than within the "magnetic propeller" model. As mentioned in Sect. 3, the basic assumptions adopted within the pulsar-like approach do not contradict any of the currently observed properties of the system, but they allow us to invoke the models developed with respect to the spin-powered pulsars for the interpretation of properties which AE Aqr shares with at least several objects of this class. Therefore, an analysis of the observed system properties within the pulsar-like approach appears to be quite reasonable.

The present state of development of both the "magnetic propeller" and the pulsar-like models is insufficient for recognizing which of these approaches is more promising. The analysis of this question is beyond the scope of the present paper. Nevertheless, to clarify the basic statements of these models we summarize the assumptions adopted within each of these approaches.

5.1. Assumptions adopted within the magnetic propeller approach

The following 6 basic assumptions, currently adopted within the magnetic propeller model, can be distinguished:

I. The dipole magnetic moment of the white dwarf is assumed to be of the order of 10^{32} G cm^3, i.e. within the expected range of the magnetic moments of Intermediate Polars.

II. The spin-down power is assumed to be transferred predominantly to the kinetic energy of the material ejected from the system due to propeller action by the white dwarf. As shown in Sect. 2.1.2, this assumption implies the mass-transfer rate in the system to be

$$\dot{M} \gtrsim 10^{18} \left(\frac{r_0}{10^{10}{\rm cm}}\right)\left(\frac{L_{\rm sd}}{6\times10^{33}{\rm erg\,s^{-1}}}\right) {\rm g\,s^{-1}}. \quad (12)$$

III. The stream of material transferred from the secondary is assumed to be strongly inhomogeneous. Actually, this assumption implies that at least 99.99% of the material is transferred in blobs. Indeed, if the mass transfer rate of the homogeneous component exceeds

$$\dot{M}_{\rm hs} \sim 10^{13}\, \eta_{0.37}^{7/2}\, \mu_{32}^{2}\, M_{0.8}^{-1/2} \left(\frac{R}{R_{\rm circ}}\right)^{-7/2} {\rm g\,s^{-1}}, \quad (13)$$

the homogeneous flow turns out to be able to reach the circularization radius and to form a disk around the magnetosphere of the white dwarf.

It should be noted that the reason for such a strong inhomogeneity is rather unclear. It might be connected with the magneto-flaring activity of the normal component or the beam instability in the region of the L1 point. At the same time, it is unlikely that it can be explained in terms of the interaction between the stream and the magnetic field of the white dwarf since at distances $R \gg R_{\rm A}$ the energy density of the magnetic field is a few orders of magnitude smaller than the thermal energy of the stream material. In particular, the solution of Arons & Lea (1980) derived for the regions $R \sim R_{\rm A}$ is obviously not applicable in this case.

IV. The temperature of blobs passing through the magnetosphere is assumed to be small enough for their contribution to the Hα emission of the system to be negligibly small. Otherwise, the presence of a high velocity loop associated with the trajectories of blobs interacting with the magnetic field of the white dwarf is expected (see Fig. 3 in Wynn et al. 1997). Such a loop, however, is not seen in the observed tomogram (for discussion see Welsh et al. 1998; Welsh 1999).

V. Almost all the blobs expelled by the white dwarf are involved in a collision process as their trajectories intersect beyond the system. Otherwise, the amount of hot material would be insufficient to explain the observed Hα emission. It should also be noted that for the observed flaring in the system to be associated with the collision of blobs, the mass transfer rate should be in excess of (see Sect. 4.3)

$$\dot{M}_{\rm b-b} \gtrsim 1.3\times10^{19}\, L_{33} \left(\frac{V_{\rm b-b}}{123{\rm km\,s^{-1}}}\right)^{-2} {\rm g\,s^{-1}}, \quad (14)$$

where L_{33} is the luminosity of the flaring component expressed in units of 10^{33} erg s^{-1} (see van Paradijs et al. 1989; Beskrovnaya et al. 1996), and the value of $V_{\rm b-b}$ is normalized to the rising velocity of flares recently derived by Skidmore et al. (2003) from high-time-resolution spectroscopy of the system. Otherwise, the energy release in the region of blobs collision turns out to be smaller than the luminosity of strong flares observed from the system.

VI. One has to assume that the blobs cool down very slowly (on a time scale of a few hours) or, for some reason, are heated again at larger distances from the system. Otherwise, the origin of the low-velocity ($\lesssim$100 km s^{-1})

component of the system Hα emission, which is seen on the observed tomogram, becomes rather unclear (see e.g. Welsh 1999; Pearson et al. 2003).

Within these assumptions a good agreement between the observed Hα Doppler tomogram and the tomogram simulated within the "magnetic propeller" model can be achieved.

5.2. Assumptions adopted within the pulsar-like white dwarf approach

The basic assumptions of the pulsar-like model of AE Aqr are as follows:

I. The dipole magnetic moment of the white dwarf is assumed to be as high as $\mu \simeq 1.4 \times 10^{34}$ G cm^3. As shown in Sect. 3, this assumption implies a rather complicated scenario for the system evolution, which invokes processes poorly investigated so far.
II. The stream of material transferred from the secondary is assumed to disintegrate into large diamagnetic blobs as it impacts onto the Alfvén surface of the primary.
III. It is assumed that the mass-transfer rate in the system varies by a factor of a few on the time scale of the orbital period. Due to these variations the structure of the tomogram changes from night to night.
IV. We have also assumed that the stream does not strongly interact with relativistic particles accelerated in the potential gap situated in the vicinity of the white dwarf surface. This implies that the opening angle of the beam of particles accelerated in the magnetic pole regions is $\theta \lesssim 18^\circ$ (here, the value of β is adopted as $\lesssim 77^\circ$, see Eracleous et al. 1994). If, nevertheless, there is interaction between the stream and the accelerated particles, the energy balance in the material of the stream should be re-calculated.

At the same time, none of the assumptions adopted within the "magnetic propeller" approach is necessary in the frame of the pulsar-like model of AE Aqr. In particular, there is no strong lower limit to the mass-transfer rate, diskless mass transfer is expected independently of whether the stream inflowing through the L1 point is homogeneous or inhomogeneous, the blobs passing the accelerating region are expected to be hot, and the low-velocity source is associated with the interaction between the magneto-dipole waves and the plasma expelled by the propeller action of the white dwarf.

6. Conclusions

We have shown that the Hα Doppler tomogram simulated within the pulsar-like white dwarf model of AE Aqr is similar to the observed tomogram in several important aspects. Namely, the emission is not centered on the white dwarf, it does not show azimuthal symmetry, and the strongest emission occurs primarily in the lower-left quadrant at velocities $\lesssim$ 500 km s^{-1}.

At least three sources of the Hα emission can be distinguished within the considered approach: (1) the emission of the stream passing through the magnetosphere of the white dwarf (the high-velocity component: 350–500 km s^{-1}); (2) the region of blob collisions (the intermediate velocity component: 200–300 km s^{-1}); and (3) the region of interaction between the stream and the magneto-dipole radiation of the white dwarf (the low-velocity component: $\lesssim$150 km s^{-1}). The relative contributions of these components to the system emission depend on the mass-transfer rate, and therefore the structure of the tomogram is expected to vary as the rate of mass transfer from the normal companion into the Roche lobe of the white dwarf changes.

The best agreement between the simulated and the observed tomograms was found assuming that the mass-transfer rate varies on a time scale of a few hours in the interval $\dot{M} \sim 10^{16}$–10^{17} g s^{-1} with the nightly mean value $\langle \dot{M} \rangle \simeq 5 \times 10^{16}$ g s^{-1}. In this case the efficiency of the propeller action by the white dwarf is limited to $0.01 \lesssim L_{\rm st}/L_{\rm sd} \lesssim 0.4$. This means that the contribution of the propeller spin-down mechanism to the observed braking of the white dwarf under the conditions of interest is small, and hence, the spin-down of the white dwarf (which is assumed to be governed by the pulsar-like spin-down mechanism) is expected to be stable independently of variations of $\dot{M}$.

Acknowledgements. We thank Dr. Chul-Sung Choi and an anonymous referee for very careful reading of the manuscript and useful comments. Nazar Ikhsanov acknowledges the support of the Alexander von Humboldt Foundation within the "Long-term Cooperation" Program. Vitaly Neustroev acknowledges the support of IRCSET under their basic research programme and the support of the HEA funded CosmoGrid project. The work was partly supported by the Russian Foundation of Basic Research under the grant 03-02-17223a and the State Scientific and Technical Program "Astronomy".

References

Arons, J., & Lea, S. M. 1980, ApJ, 235, 1016
Bastian, T. S., Dulk, G. A., & Chanmugam, G. 1988, ApJ, 324, 431
Becker, W., & Trümper, J. 1997, A&A, 326, 682
Beskrovnaya, N. G., Ikhsanov, N. R., Bruch, A., & Shakhovskoy, N. M. 1996, A&A, 307, 840
Bowden, C. C. G., Bradbury, S. M., Chadwick, P. M., et al. 1992, Astropart. Phys., 1, 47
Bruch, A. 1991, A&A, 251, 59
Chanmugam, G. 1992, ARA&A, 30, 143
Chanmugam, G., Meenakshi, R., & Tohline, J. E. 1987, ApJ, 319, 188
Chincarini, G., & Walker, M. F. 1981, A&A, 104, 24
Choi, C.-S., Dotani, T., & Agrawal, P. C. 1999, ApJ, 525, 399
Choi, C.-S., & Yi, I. 2000, ApJ, 538, 862
Clayton, K. L., & Osborne, J. P. 1995, in Magnetic Cataclysmic Variables, ed. D. Buckley, & B. Warner, ASP Conf. Ser., 85, 379
Cropper, M. 1990, Space Sci. Rev., 54, 195
de Jager, O. C., Meintjes, P. J., O'Donoghue, D., & Robinson, E. L. 1994, MNRAS, 267, 577
Eracleous, M., & Horne, K. 1996, ApJ, 471, 427
Eracleous, M., Horne, K., Robinson, E. L., et al. 1994, ApJ, 433, 313
Frank, J. F., King, A. R., & Raine, D. J. 1985, Accretion power in Astrophysics (Cambridge: Cambridge University Press), 60
Friedjung, M. 1997, New Astron., 2, 319
Goldreich, P., & Julian, W. H. 1969, ApJ, 157, 869

Hameury, J.-M., King, A. R., & Lasota, J.-P. 1986, MNRAS, 218, 695
Hartmann, D. H. 1995, A&AR, 6, 225
Ikhsanov, N. R. 1997, A&A, 325, 1045
Ikhsanov, N. R. 1998, A&A, 338, 521
Ikhsanov, N. R. 1999, A&A, 347, 915
Ikhsanov, N. R. 2001, A&A, 374, 1030
Ikhsanov, N. R., Jordan, S., & Beskrovnaya, N. G. 2002, A&A, 385, 152
Ikhsanov, N. R., & Beskrovnaya, N. G. 2002, ApJ, 576, L57
Jordan, S. 2001, in White Dwarfs, ed. J. L. Provencal et al., ASP Conf. Ser., 226, 269
Kluźniak, W., & Ruderman, M. 1998, ApJ, 505, L113
Lang, M. J., Buckley, J. H., Carter-Lewis, D. A., et al. 1998, Astroparticle Physics, 9, 203
Manchester, R. N., & Taylor, J. H. 1977, Pulsars (San Francisco: Freeman)
Meintjes, P. J. 2002, MNRAS, 366, 265
Meintjes, P. J., de Jager, O. C., Raubenheimer, B. C., et al. 1994, ApJ, 434, 292
Meintjes, P. J., & de Jager, O. C. 2000, MNRAS, 311, 611
Meintjes, P. J., & Venter, L. A. 2003, MNRAS, 341, 891
Michel, F. C. 1991, Theory of Neutron Star Magnetospheres (University of Chicago Press)
Pacini, F. 1968, Nature, 219, 145
Paczyński, B. 1990, ApJ, 365, L9
Patterson, J. 1979, ApJ, 234, 978
Patterson, J., Branch, D., Chincarini, G., & Robinson, E. L. 1980, ApJ, 240, L133
Pearson, K. J., Horne, K., & Skidmore, W. 2003, MNRAS, 338, 1067
Rees, M. J., & Gunn, J. E. 1974, MNRAS, 167, 1
Reinsch, K., & Beuermann, K. 1994, A&A, 282, 493
Reinsch, K., Beuermann, K., Hanusch, H., & Thomas, H.-C. 1995, in Magnetic Cataclysmic Variables, ed. D. Buckley, & B. Warner, ASP Conf. Ser., 85, 115
Schenker, K., King, A. R., Kolb, U., et al. 2002, MNRAS, 377, 1105
Skidmore, W., O'Brien, K., Horne, K., et al. 2003, MNRAS, 338, 1057
Spruit, H. 1999, A&A, 341, L1
Stockman, H. S., Schmidt, G. D., Berriman, G., et al. 1992, ApJ, 401, 628
Tompson, D. J. 1996, in Pulsars: Problems & Progress, ed. S. Johnston, M. A. Walker, & M. Bailes, ASP Conf. Ser., 105, 307
van Paradijs, J., Kraakman, H., & van Amerongen, S. 1989, A&AS, 79, 205
Warner, B. 1995, Cataclysmic Variable Stars (Cambridge University Press)
Welsh, W. F. 1999, Annapolis Workshop on Magnetic Cataclysmic Variables, ed. C. Hellier, & K. Mukai, ASP Conf. Ser., 157, 357
Welsh, W. F., Horne, K., & Gomer, R. 1995, MNRAS, 275, 649
Welsh, W. F., Horne, K., & Gomer, R. 1998, MNRAS, 298, 285
Wynn, G. A., & King, A. R. 1995, MNRAS, 275, 9
Wynn, G. A., King, A. R., & Horne, K. 1997, MNRAS, 286, 436